Spatially Correlated Charge Transport in Organic Thin Film Transistors

Franco Dinelli, Mauro Murgia, Pablo Levy,* Massimiliano Cavallini, and Fabio Biscarini†

Consiglio Nazionale delle Ricerche—Istituto per lo Studio dei Materiali Nanostrutturati-Sezione Bologna, Via P. Gobetti 101, I-40129 Bologna Italy

Dago M. de Leeuw

Philips Research Laboratory, Prof. Holstlaan 4, 5656 AA Eindhoven, The Netherlands

(Received 4 March 2002; revised manuscript received 6 August 2003; published 19 March 2004)

Hole mobility in organic ultrathin film field-effect transistors is studied as a function of the coverage. For layered sexithienyl films, the charge carrier mobility rapidly increases with increasing coverage and saturates at a coverage of about two monolayers. This shows that the first two molecular layers next to the dielectric interface dominate the charge transport. A quantitative analysis of spatial correlations shows that the second layer is crucial, as it provides efficient percolation pathways for carriers generated in both the first and the second layers. The upper layers do not actively contribute either because their domains are smaller than the ones in the second layer or because the carrier density is negligible.

DOI: 10.1103/PhysRevLett.92.116802 PACS numbers: 73.61.Ph, 68.37.–d, 68.55.–a, 81.07.Nb

The mechanism of charge transport in organic field-effect transistors (FETs), where a thin film of conjugated molecules acts as the semiconductor layer, is still a challenging problem. Since the demonstration of organic FETs [1–3], the charge carrier mobility μ at room temperature (RT) has increased from 10^{-4}–10^{-5} up to a few cm^2/Vs [4,5]. In organic single crystals, μ is $\sim$1–10 cm^2/Vs at RT and increases with decreasing temperature [6,7], as a result of charge coherent motion due to long-range molecular order. In thin film transistors, μ is usually one or two orders of magnitude smaller and decreases with decreasing temperature. Transport in thin films is governed by hopping through energy-disordered localized sites [8], and the discrepancy may arise from partial disorder, structural defects, traps, or imperfect interfaces with the electrodes [9–12]. In order to understand the crossover from thin film to single crystal transport, it is crucial to experimentally control the structure and morphology of the accumulation layer in a FET. Continuum electrostatic models predict that the accumulation layer resides within one or a few molecular layers in contact with the gate dielectric [11]. Few experimental studies have addressed the nature of the accumulation layer in FETs with thin films of different thicknesses [13] and single domains [14]. No conclusive evidence of a thickness effect on charge mobility has been reported.

In this Letter, we show that, in ultrathin films of sexithienyl grown in a molecularly ordered layer-by-layer fashion, μ is a rapidly increasing function of coverage Θ and saturates at a plateau upon completion of the second layer. This demonstrates that (i) charge carrier mobility has a length scale dependence and (ii) only the first two molecular layers next to the dielectric interface contribute to the charge transport. The physical size of the transport layer, which may not necessarily coincide with the accumulation layer, is discussed in terms of the spatial correlations between layers.

We investigate charge carrier mobility in sexithienyl FETs where film thickness was systematically varied. FET test devices were fabricated from heavily n-type doped Si wafers that act as a common gate contact. A 200-nm thin insulating layer of SiO_2 was thermally grown and passivated by hexamethyldisilazane. The gate capacitance per unit area C_i is 17 nF/cm^2. Interdigitated source and drain Au/Ti electrodes were made by photolithography with channel length L and width W ranging from 1 to 40 μm and 10^3 to 2×10^4 μm, respectively.

Sexithienyl thin films are grown on the FET substrates by sublimation in an organic molecular beam apparatus (10^{-10} mbar base pressure). Deposition rate F is monitored with a quartz oscillator. Two sets of samples are reported here: one termed high rate (HR) obtained at constant deposition temperature $T = 150\,^{\circ}C$ and $F = 0.6$ nm/min; the other, low rate (LR) at $T = 120\,^{\circ}C$ and $F = 0.12$ nm/min. Both conditions yield layered growth on the dielectric substrate, with sexithienyl molecules oriented normal to it [15,16]. In this regime, scaling properties can be renormalized by the ratio between molecular self-diffusivity $D \propto \exp(-E_d/k_bT)$ and F [17]. For sexithienyl, $E_d \approx 0.3$–0.4 eV [15,18], so D/F of the HR series is 2–3 times smaller than D/F of the LR series. Film thickness is proportional to coverage Θ expressed in monolayer (ML) units and is measured from atomic force microscopy (AFM) images [19]. For sexithienyl 1 ML $\approx$ 2.4 nm, and Θ is varied between 0.1 and 10 ML.

The p-type sexithienyl FETs are operated in accumulation in air. Devices were also measured in vacuum (10^{-3} mbar) after annealing for 1 h at 90 °C. In air we observe a +8 to +10 V turn-on voltage V_t (consistent with [13(b)]), and a slight hysteresis that disappears in vacuum [20]. In Fig. 1(a) the transfer characteristics of LR

films show saturation at high gate voltage and a small hysteresis that decreases with increasing coverage. LR devices are more stable in time and upon repeated operations with respect to HR ones. The mobility is extracted from the transfer characteristics at fixed $V_g = -20$ V and $L = 40$ μm [21] and plotted in Fig. 1(b) as a function of Θ. For the HR series, as $\Theta < 1.5$ ML, μ rises as a power law with an exponent equal to 2.4 ± 0.02. For $1.5 < \Theta < 2$ ML, μ rises faster with an exponent $\approx 6.5 \pm 2.8$. As $\Theta \geq 2$ ML, μ reaches a plateau whose mean value is $\mu_{HR} = 0.015$ cm^2/Vs. For the LR series, the trend is similar, but μ is always larger than the HR values and saturates at $\mu_{LR} = 0.043$ cm^2/Vs for $\Theta \geq 1.3$ ML. Saturated μ values compare with the largest charge mobilities reported for sexithienyl transistors (0.15 cm^2/Vs in single crystal [22] and 0.02–0.03 cm^2/Vs in thin film FETs [4]). We infer that the FET current is sustained by the first two layers, while the upper layers do not effectively contribute to transport. This is the first direct evidence of the physical thickness of the transport layer in organic thin film transistors.

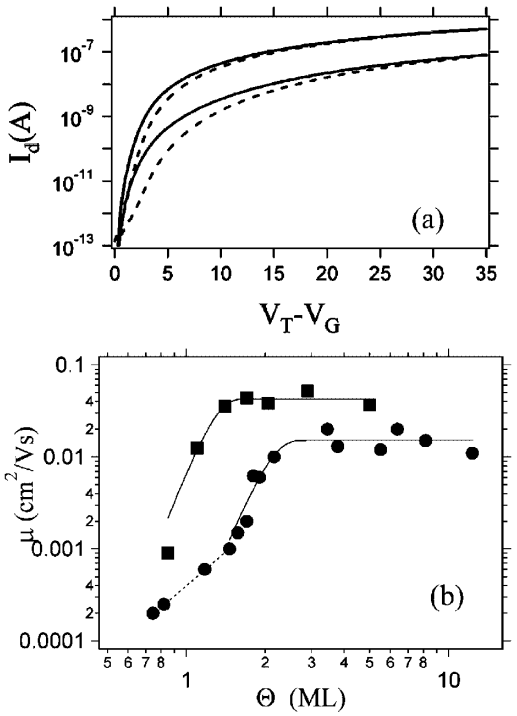

FIG. 1. (a) Transfer curves at $V_d = -1$ V for LR films with coverage of 1.1 (lower curves) and 3 ML (upper curves). Mobility is extracted at $V_g = -20$ V. Solid and dashed lines are forward and backward gate sweeps, respectively. (b) Hole mobility versus coverage. The solid line is the fitting function $\mu \cong \mu_{sat}\{1 - \exp[-(\Theta/\Theta_c)^\alpha]\}$ yielding plateau μ_{sat}, crossover coverage Θ_c, and exponent α. For HR series (circles), $\mu_{sat} = 0.015(\pm 0.001)$ cm^2/Vs, $\Theta_c = 2.1(\pm 0.1)$ ML, and $\alpha = 6.5(\pm 2.8)$. The dashed line is the power law fit to submonolayer mobility with $\alpha = 2.4(\pm 0.02)$. For LR series (squares), $\mu_{sat} = 0.043(\pm 0.003)$ cm^2/Vs, $\Theta_c = 1.29(\pm 0.07)$ ML, and $\alpha = 7.1(\pm 2.9)$.

We compare the evolution of mobility with that of the morphology. For HR films (Fig. 2, left column) at $\Theta \leq 0.5$ ML, monolayer islands nucleate and grow on the dielectric surface. At $\Theta = 0.7$ ML the islands have coalesced, forming a network. As the first layer is completed ($\Theta = 1.1$ ML), nucleation of the second layer starts. The density of nuclei at the second layer is smaller than in the first layer. At $\Theta \geq 1.5$ ML the islands of the second layer are substantially larger than the ones in the first layer. The third layer nucleates before the completion of the second layer. An increasing number of islands nucleates in the upper layers as $\Theta > 2$ ML: at $\Theta \approx 2.2$ ML, the fifth layer; $\Theta = 3.5$ ML, the seventh layer. The stacking of monolayer terraces makes islands grow progressively more 3D. The thickness of each layer $\Delta h = 2.4 \pm 0.3$ nm from AFM matches the crystallographic value (half of the a axis is 2.27 nm in powders, 2.43 nm in single crystals) [23,24]. Molecules retain their out-of-plane orientation with their long axis almost normal to the surface.

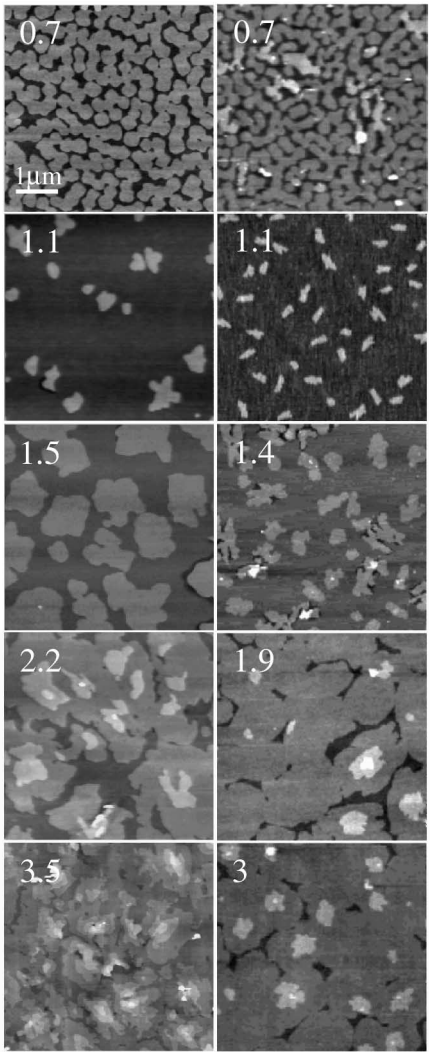

FIG. 2. Evolution of sexithienyl film morphology for increasing coverage: (left column) HR and (right column) LR series.

In the case of LR films (Fig. 2, right column), the nucleation density on the dielectric substrate is comparable to that of the HR films, while the nucleation density of the second layer is higher. Above 2 ML, the layers keep on forming with the island-nucleation-and-growth mechanism up to, at least, a coverage of 6 ML. This is clear from the comparison of the morphology at $\Theta \approx 2$ and 3 ML.

The evolution of the morphology has been analyzed by means of the surface roughness w, which is the root mean square fluctuation of the film topography h, and the correlation length ξ of the height fluctuations that represents the characteristic length scale [18]. Image scan size was fixed at 10 μm. At this length scale, larger than ξ, w is scale invariant [17,18]. For a layered morphology, w describes the out-of-plane disorder with respect to the homogeneous layer, and is expressed as

$$w = \sqrt{\langle h^2 \rangle - \langle h \rangle^2} = \Delta h \{[2\bar{n}(\Theta) - 1 - \Theta]\Theta\}^{1/2}. \quad (1)$$

The mean layer number $\bar{n}(\Theta) = \sum_{i=1}^{n} i(\Theta_i/\Theta)$ depends on the distribution of layers that is determined by the growth mechanism. In layer-by-layer growth, only the uppermost nth layer contributes to w. Since $\Theta_i = 1$ for $i < n$ and $\Theta_n = 1 - n + \Theta$, Eq. (1) becomes

$$w = \Delta h[(2n - 1)\Theta - n(n - 1) - \Theta^2]^{1/2}. \quad (2)$$

Figure 3(a) shows w versus coverage Θ. The roughness evolution of the first monolayer is in remarkable agreement with Eq. (2) for $n = 1$, viz. $w = \Delta h[\Theta(1 - \Theta)]^{0.5}$. In the case of the HR films, layer-by-layer growth continues also for the second layer, albeit as $1.5 < Q <$ 2 ML, w overshoots the ideal values and changes abruptly as $\Theta \approx 2$ ML. Onset of power-law scaling with $w \approx \Theta^{0.42(\pm 0.03)}$ is established at $\Theta > 2$ ML. This is consistent with the roughness scaling behavior expected for a system governed by the Schwöbel barrier, viz. $w \approx \Theta^{\beta} < \Theta^{0.5}$ [25]. At $\Theta = 2.2$ ML the contribution of the first two layers to total coverage is $\Theta_1 = 0.99$ ML and $\Theta_2 =$ 0.91 ML, respectively, while for larger Θ, upper layers contribute more than 30% of the total coverage. Thus, for the HR series, a roughening transition from 2D to 3D growth coincides with the onset of saturation of the charge carrier mobility. In the case of the LR films at high coverage, w takes values in the range consistent with layer-by-layer growth.

Figure 3(b) shows the correlation length ξ extracted from AFM images using the analysis of the topographical power spectrum density [18]. Noticeably, the maximum ξ is reached at the coverage Θ between 1 and 2 ML, then it decreases for the HR films or remains constant for the LR films. This implies that the islands of the second layer are larger than the islands in the first layer and, hence, they extend across the domain boundaries of the first layer. The size of the islands of the third and upper layers is smaller than or comparable to that of the islands in the second layer.

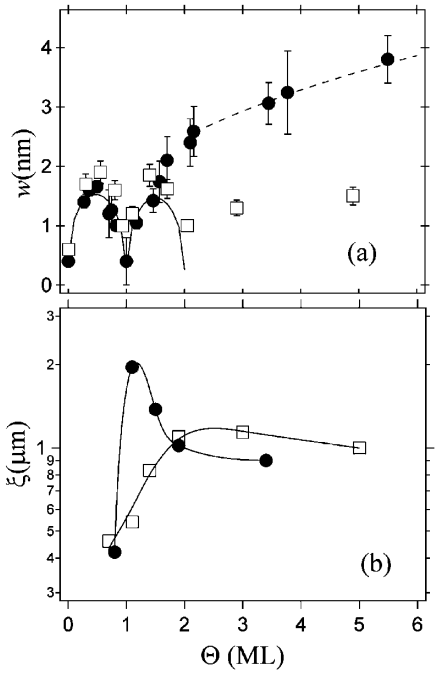

FIG. 3. (a) Saturated roughness vs coverage. The solid line is Eq. (2); the dashed line is a power-law fit with exponent $\beta = 0.42 \pm 0.03$. The roughness of the bare substrate ($\Theta = 0$ ML) is added as an offset to Eq. (2); (b) correlation length vs coverage; solid lines are guides to the eye. Circles and squares are data of HR and LR series, respectively.

The combined evidence on μ and morphology allows us to infer that, in layered organic thin film transistors, charge transport is governed by percolation across the first layer and mediated by the second layer. In the formation of the first layer, coverage and domain boundaries between coalescing islands determine the percolation pathways. By assuming that μ scales like the conductivity versus coverage in a percolation problem, then a power law with exponent $\alpha = 1$–1.4 for percolation in 2D and $\alpha = 1.5$–2 in 3D should be expected [26,8]. For $\Theta <$ 1 ML the geometry-corrected exponent is $\alpha \approx 2.4 - 1 =$ 1.4 [27], consistently with percolation scaling in 2D. Noticeably, for $1 < \Theta < 1.5$ ML the mobility increases when the second layer is not yet connected through the channel. This implies that the islands of the second layer provide additional paths for the carriers generated in the first layer by bridging across domain boundaries of the first layer. Charge transport across stacked layers is not relevant in oligothienyl crystals due to the weaker coupling between molecules in adjacent molecular planes. In thin films, instead, the probability of the charge being transferred from one layer to an adjacent one is modulated by the transport rate across domain boundaries of the first layer and enhanced by the fact that the contact area between first and second layer is large compared to the longitudinal cross section. Such mechanism of interlayer transport becomes less important when a few domain boundaries are present in the first layer. Comparison

between LR and HR series indeed suggests that the role of the second layer diminishes when the molecular order in the first layer increases. This might be indeed the case of the experiment reported in Ref. [14] and in single crystal transistors. Layers above the second one do not significantly contribute to percolation, because they are either largely incomplete (as in HR series) or because their domain size is smaller.

A final consideration concerns the charge distribution in ultrathin films. Based on the Poisson equation for a continuous, semi-infinite, isotropic semiconductor, the Debye length (that quantifies the size of the accumulation layer) of sexithienyl films was expected to be comparable to the thickness of one monolayer [11]. This implies that a negligible charge carrier density is generated in the upper layers. The increase of the experimental exponent from $\alpha \approx 2.4$ to $\alpha \approx 6$–7 cannot be accounted for solely by the increased dimensionality of the active layer. This strongly hints that a relevant carrier density is generated in the second layer and transported as this layer becomes more and more connected. Modeling of the charge distribution in the accumulation layer should take into account the anisotropic dielectric permittivity, finite thickness, and layered architecture. Substantial carrier density may also be present also in layers above the second one [28]; however, it does not contribute to charge transport because of unfavorable spatial correlations. Thus, transport and accumulation layers may not necessarily coincide.

In conclusion, the spatial correlations at different length scales, from intermolecular distances to the channel length, play a crucial role on the transport mechanism in layered thin films. This, together with the fact that charge density is generated also in upper layers, suggests that charge mobility can be enhanced by tailoring length scales and stacking sequence of the molecular layers.

We thank J.-F. Moulin, C. Taliani, G. Cardinali, U. Valbusa, L. Molenkamp, V. Wagner, G. Horowitz. This work is supported by EU G5RD-CT2000-00349 MONALISA. P. L. was supported by ICTP-TRIL.

*Permanent address: Departamento de Fisica, Centro Atómico Constituyentes, CNEA, Buenos Aires, Argentina.
†Electronic address: f.biscarini@ism.bo.cnr.it

[1] A. Tsumura, H. Koezuka, and T. Ando, Appl. Phys. Lett. **49**, 1210 (1986).
[2] G. Horowitz *et al.*, Solid State Commun. **72**, 381 (1989).
[3] P. Ostoja *et al.*, Synth. Met. **54**, 447 (1993).
[4] (a) C. D. Dimitrakopoulos and D. J. Mascaro, IBM J. Res. Dev. **45**, 11 (2001); (b) D. Fichou, *Handbook of Oligo- and Polythiophenes* (Academic, New York, 1998), p. 271.
[5] S. F. Nelson *et al.*, Appl. Phys. Lett. **72**, 1854 (1998).
[6] N. Karl, in *Organic Electronic Materials Conjugated Polymers and Low Molecular Weight Organic Solids*, edited by R. Farchioni and G. Grosso, Springer Series in Materials Science Vol. 41 (Springer-Verlag, Berlin, 2000), p. 283.
[7] M. Pope and C. E. Swenberg, *Electronic Processes in Organic Crystals and Polymers* (Oxford University Press, New York, 1999), 2nd ed., p. 337–340.
[8] H. Bässler, Phys. Status Solidi B **175**, 15 (1993).
[9] M. C. J. M. Vissenberg and M. Matters, Phys. Rev. B **57**, 964 (1998).
[10] S. V. Novikov *et al.*, Phys. Rev. Lett. **81**, 4472 (1998).
[11] G. Horowitz *et al.*, Adv. Mater. **10**, 923 (1998).
[12] G. Horowitz, R. Hajlaoui, and F. Kouki, Eur. Phys. J. Appl. Phys. **1**, 361 (1998).
[13] (a) A. Dodalabapur, L. Torsi, and H. E. Katz, Science **268**, 270 (1995); (b) H. G. O. Sandberg *et al.*, Langmuir **18**, 10176 (2002).
[14] E. L. Granstrom and C. D. Frisbie, J. Phys. Chem. B **103**, 8842 (1999).
[15] F. Biscarini *et al.*, Phys. Rev. B **52**, 14868 (1995).
[16] M. Muccini *et al.*, Adv. Mater. **13**, 355 (2001).
[17] A.-L. Barabàsi and H. E. Stanley, *Fractal Concepts in Surface Growth* (Cambridge University Press, Cambridge, England, 1995).
[18] F. Biscarini *et al.*, Phys. Rev. Lett. **78**, 2389 (1997).
[19] For a layered morphology, the mean height $\langle h \rangle$ with respect to the background is proportional to Θ: $\langle h \rangle = \frac{1}{A}\sum_{i=1}^{n} \Delta h_i A_i = \sum_{i=1}^{n} \Delta h_i \Theta_i \approx \Delta h \Theta$, where A is the area of the AFM image, and Δh_i and Θ_i are step height and coverage of the ith layer. $\langle h \rangle$ is evaluated pixel by pixel on 500×500 pixel images corrected for slope. By thresholding analysis (NIH-Image, NIH, Bethesda, MD), we extract Δh_i, Θ_i, and Θ. The right side approximation holds for $\Delta h = 2.4 \pm 0.3$ nm, which is the thickness of a sexithienyl monolayer measured by AFM.
[20] E. J. Meijer *et al.*, Appl. Phys. Lett. **82**, 4576 (2003).
[21] Mobility μ depends on the gate voltage, and we used two methods to extract it: in the linear regime at a drain bias of -1 V, as $\mu_{\mathrm{lin}}(V_g) = (L/WC_iV_d)\delta I_d/\delta V_g$, and in the saturation regime, $V_d < V_g < 0$, as $\mu_{\mathrm{sat}}(V_g) = (L/WC_i)\delta^2 I_d/\delta^2 V_g$ [G. Horowitz *et al.*, J. Appl. Phys. **67**, 381 (1990)], or alternatively $\mu_{\mathrm{sat}}(V_g) = (2L/WC_i) \times (\delta\sqrt{I_d}/\delta V_g)^2$ [D. J. Gundlach *et al.*, Appl. Phys. Lett. **71**, 3853 (1997)]. Since values were comparable, we report μ_{lin} data.
[22] G. Horowitz, M. E. Hajlaoui, and R. Hajlaoui, J. Appl. Phys. **87**, 4456 (2000).
[23] W. Porzio, S. Destri, M. Mascherpa, and S. Brückner, Acta Polym. **44**, 266 (1993).
[24] G. Horowitz *et al.*, Chem. Mater. **7**, 1337 (1995).
[25] M. C. Bartelt and J. W. Evans, Phys. Rev. Lett. **75**, 4250 (1995).
[26] B. I. Shklovskii and A. L. Efros, *Electronic Properties of Doped Semiconductors* (Springer-Verlag, Berlin, 1984).
[27] At $\Theta < 1$ the channel is partially covered, so the effective area of the channel depends roughly on Θ as $A_{\mathrm{eff}} \approx WL\Theta$. In this range of Θ, μ should then be rescaled by Θ^{-1}.
[28] G. Horowitz (private communication).